Cell Biochem Biophys (2013) 67:537–546
DOI 10.1007/s12013-013-9539-2

ORIGINAL PAPER

Effect of miR-21 on Renal Fibrosis by Regulating MMP-9 and TIMP1 in kk-ay Diabetic Nephropathy Mice

Jinyang Wang · Yanbin Gao · Mingfei Ma · Minzhou Li · Dawei Zou · Jinkui Yang · Zhiyao Zhu · Xuan Zhao

Published online: 27 February 2013

Abstract MicroRNAs (miRs) play important roles in initiation and progression of many pathologic processes. However, the roles of miRs in diabetic nephropathy remain unclear. This study was to determine whether miR-21 was involved in diabetic nephropathy and to explore the relationship between miR-21 and MMP9/TIMP1 expression in diabetic nephropathy. In situ hybridization studies showed that miR-21 was primarily localized and distributed in cortical glomerular and renal tubular cells in diabetic kk-ay kidney. Real-time quantitative RT-PCR demonstrated that the expression of miR-21 was significantly increased in kk-ay mice, compared with control C57BL mice. Interestingly, miR-21 expression positively correlated with urine albumin creatine ratio (ACR), TIMP1, collagen IV (ColIV), and fibronectin (FN); while negatively correlated with creatine clearance ratio (Ccr) and MMP-9 protein. Importantly, antagomir-21 not only ameliorated Ccr and ACR but also decreased TIMP1, ColIV, and FN proteins. In conclusion, our data demonstrate that miR-21 contributes to renal fibrosis by mediating MMP9/TIMP1 and that inhibition of miR-21 may be a novel target for diabetic nephropathy.

Keywords miRNA · ECM · MMP-9 and TIMP-1 · ACR · Ccr · Diabetic nephropathy

J. Wang · Y. Gao · D. Zou · Z. Zhu · X. Zhao
School of Traditional Chinese Medicine, Capital Medical University, Beijing, People's Republic of China

J. Wang · J. Yang
Department of Endocrinology, Beijing Tongren Hospital, Capital Medical University, Beijing, People's Republic of China

J. Wang
Department of Endocrinology and Metabolism, Capital Medical University, Beijing, People's Republic of China

Y. Gao (✉)
Chinese Medical College, Capital Medical University, #10, Youanmenwai Xitoutiao, Fengtai District, Beijing 100069, People's Republic of China
e-mail: gaoyb111@yahoo.com.cn

M. Ma · M. Li
Department of Endocrine, Beijing University of Chinese Medicine, Beijing, People's Republic of China

Introduction

Diabetic nephropathy is one of the most important diabetic microangiopathies. Diabetic patients with end-stage kidney disease have a 5-year survival of only 20 % [1]. One key feature of diabetic nephropathy (DN) is the accumulation of extracellular matrix proteins (ECMs) such as collagen and fibronectin (FN) [2]. The ECM is regulated by matrix metalloproteinases (MMPs) and their tissue inhibitors of metalloproteinase (TIMPs) [3].

The kk-ay mouse is considered suitable as a polygenic model for human type-2 diabetes mellitus and is produced by transferring the yellow obese gene (A^y allele) into the kk/Ta mice. The kk-ay mouse develops marked high glucose, albuminuria, and renal fibrosis with renal lesions histopathologically resembling human DN [4].

MicroRNAs (miRs) are endogenous non-coding RNA molecules, 20–22 nucleotides in length; they are a class of small regulatory RNAs that silence messenger RNAs by binding to their 3′-untranslated regions (UTRs). By inhibiting target genes expression, miRs have been reported to modulate a variety of physiological and pathological processes by inducing mRNA degradation or inhibiting protein translation, including cell differentiation, proliferation, apoptosis, and metabolism [5]. Although miRNA

studies predominate in the cancer fields, little is known about their expression patterns or role in other diseases, especially for DN. Recently, it has been reported that miRs play a role in diabetes mellitus and its complications. For example, it is found that the pancreatic islet-specific miRNA [6], miR-375, decreases insulin secretion, and is a key determinant of blood homeostasis [7, 8]. miR-30d is up-regulated by glucose, increases insulin gene expression [9]. MiR-29 aggravates insulin resistance and inhibits fibrosis [10, 11]. miR-192 may be a critical downstream mediator of TGF-β/Smad3 signaling in the development of renal fibrosis [12]. MicroRNA-377 is up-regulated and can lead to increased FN production in DN [13]. MicroRNA-451 regulates p38 MAPK signaling by targeting of Ywhaz and suppresses the mesangial hypertrophy in early DN [14]. MiR-133 promotes diabetic cardiopathy by inhibiting kalium ion channel of ERG gene, indicating the participation of miRs in diabetes mellitus and its complications [15]. Furthermore, it has been reported that miR-21 plays a role in the regulation of MMPs and TIMPs expression in cancers [16–19]. However, the effect of miR-21 on ECMs production of DN remains unclear.

The aim of this study was to identify whether miR-21 was involved in renal fibrosis of DN and to explore the relationship between miR-21 and MMP9/TIMP1 expression. The results suggest that miR-21 can promote renal fibrosis through regulating MMP9 and TIMP1 expression, and that inhibition of miR-21 may be a novel therapeutic target to attenuate renal fibrosis.

Materials and Methods

Animals Models

The study protocol was approved by the Institutional Animal Care and Use Committee at Capital Medical University and in accordance with the National Institutes of Health Guide for the Care and Use of Laboratory Animals. Male C57BL/6 J (8 weeks of age, 10 mice) and kk-ay mice (8 weeks of age, 20 mice) from Chinese Academy of Medical Sciences (Beijing, China) were individually housed in plastic cages with free access to food and water throughout the experiment. All mice were maintained in the same room under conventional conditions with a regular 12-h light/dark cycle with the temperature controlled at 24 ± 1 °C. C57BL/6 J mice (control group) were fed by common forage, kk-ay mice were fed by research diets. After 4 weeks of feeding, random blood glucose (RBG) in the blood collected from tail vein of each animal was checked by a portable glucometer, C57BL/6 J mice were classified as normal control (C57BL group = 10), kk-ay mice were considered DN when their RBG was ≥300 mg/dL (16.7 mmol/L) and urine albumin creatine ratio (ACR) was ≥300 μg/mg. kk-ay mice were then randomly divided into DN control group (kk-ay group, $n = 10$), which were intraperitoneally injected with vehicle and DN treatment group (antagomir-21 group = 10), which were intraperitoneally injected with antagomir-21 (the antagonist of miR-21, 30 mg/kg day, Ribobio, China) for 8 weeks. Antagomir is a miRNA antagonist, which binds with mature miRNA in the body. Antagomir prevents miRNA and its target gene mRNA complementary pairing, and restrains the action of miRNA [18]. Renal cortical tissue from each mouse was divided into three parts, one was immediately frozen in liquid nitrogen for later use, and another two parts were fixed with 2 % glutaraldehyde and 4 % paraformaldehyde for electron microscope and light microscopy, respectively.

Biochemical Characterizations

The level of fasting serum creatine and fasting body weight were measured at 8, 16, and 20 weeks of age. The urine samples were collected for a period of 24 h using a mouse metabolic cage (CLEA Japan). The 24-h urine collected from each diabetic mouse and control was then centrifuged at 2,000 rpm for 10 min. HbA1c, urinary albumin, and creatinine were measured by immunoassay (DCA 2000 system, Siemens AG, Munich, Germany). All analyses were performed in accordance with the manuals provided by the manufacturers. The urinary albumin excretion rate was calculated as: ACR = urinary albumin (μg)/urinary creatine (mg). Creatine clearance ratio (Ccr) was calculated using the following equation: Ccr (mL/min kg) = [urinary Cr (mg/dL) × urinary volume (mL)/serum Cr (mg/dL)] × [1,000/body weight (g)] × [1/1,440 (min)].

Light and Electron Microscopy

Tissue for light microscopy was fixed in 10 % phosphate-buffered formalin and then embedded in paraffin. Four-micrometer thick sections were processed for hematoxylin–eosin and Masson's trichrome staining by light microscopy. Morphologic analyses were performed by an experienced pathologist who was blinded to the source of the tissue. The extent of glomerular sclerosis was assessed by a semi-quantitative analysis as described by Li et al. [20]. At least 40 glomeruli from each kidney were graded on the hematoxylin–eosin and Masson's trichrome-stained sections according to the following criteria: 0, no sclerosis; 1, <25 % cross-sectional sclerosis; 2, 25–50 % exhibiting sclerosis; 3, 50–75 % exhibiting sclerosis; and 4, >75 % cross-sectional sclerosis. The glomerular sclerosis index (GSI) for each mouse was calculated as follows: (N1 × 1 + N2 × 2 + N3 × 3 + N4 × 4)/n, where N1, N2, N3, and N4 represent the numbers of glomeruli that exhibited grades 1, 2, 3, and 4,

respectively, and n represents the number of glomeruli assessed [21]. The scale for each mouse was reported as the mean of 20 random high-power (400×) fields per section. Tissues for electron microscope were fixed with 2 % glutaraldehyde in 0.1 mol/L phosphate buffer at 4 °C for 120 min. They were then sectioned using a regular diamond knife into ultrathin sections. Ultrathin sections were collected on 100-mesh copper grids and double stained with 4 % uranyl acetate and lead citrate. The sections were examined with a Hitachi 7100 transmission electron microscope (Hitachi High Technologies, Tokyo, Japan) operated at 75 kV.

In Situ Hybridization

In situ hybridization (ISH) for miR-21 was performed using double-digoxigenin-labeled LNAmiRCURY probes (Exiqon, Vedbaek, Denmark) as described previously [22]. Briefly, 5-μm sections of FFPE kidney tissue were deparaffinized by sequential washes with xylene, 100–25 % ethanol, and PBS. The sections were deproteinated with proteinase K and fixed with 4 % paraformaldehyde. Prehybridization was performed with hybridization buffer [50 % formamide, 5× SSC, 0.1 % Tween 20, 50 μg/mL heparin, and 500 μg/mL yeast tRNA (pH 6)]. Hybridization was performed with digoxigenin (Dig)-conjugated miR-21 probes (Exiqon, the sequence of double-digoxigenin-labeled specific miR-21 probe: 5′–3′/5DigN/TCAACATCA GTCTGATAAGCTA/3Dig-N/) or Dig-conjugated control probes with scrambled sequence (Exiqon) with concentration of 20 nM in hybridization buffer for 12 h at 62 °C. The sections were washed with 2× SSC, then multiple washes in 50 % formamide, 2× SSC, and finally PBS and 0.1 % Tween 20. The sections were blocked with blocking buffer (2 %sheep serum, 2 mg/mL BSA in PBS, and 0.1 % Tween 20) and then incubated with anti-digoxigenin-alkaline phosphatase (Roche, Mannheim, Germany) in blocking buffer for 12 h. The sections were washed repeatedly in PBS and 0.1 % Tween 20, and detection was performed using 1-step NBT/BCIP plus Suppressor (Pierce) according to manufacturer's instructions, with light blue cytoplasmic staining being positive. The sections were double stained with fast red to manifest nuclei.

Real-Time RT-PCR Analysis

Total RNA from tissue and cells were isolated using TRIzol reagent (Invitrogen) to obtain both miRNA and mRNA. For analysis of miR-21 expression, the stem-loop RT primer, real-time PCR primers, and TaqMan MGB probe were designed as described previously [23]. Briefly, miRs were reverse transcribed into cDNAs by SuperScript II reverse transcriptase. Real-time PCR was performed using a standard TaqMan PCR protocol according to manufacturer's protocols (Applied Biosystems), and relative expression was calculated using the $2^{-\Delta\Delta Ct}$ method [24] and normalized to the expression of U6 RNA. Relative mRA levels of TIMP1, MMP-9, FN, and collagen IV (ColIV) were examined by SYBR green real-time quantitative reverse transcription PCR (qRT-PCR) (Applied Biosystems) and normalized to β-actin mRNA. The sequences of TIMP-1 mRNA and MMP-9 are the following—TIMP-1: forward primer 5′-tccccagaaatcatcgagac-3′, reverse primer 5′-atggctgaacagggaaacac-3′; MMP-9: forward primer 5′-gac tcggtctttgaggagcc-3′, reverse primer 5′-gaactcacgcgccagta gaa-3′; FN: forward primer 5′-tctgggaaatggaaaaggggaatgg-3′, reverse primer 5′-cactgaagcaggtttcctcggttgt-3′; ColIV: forward primer 5′-tggtcttactgggaactttgctgc-3′; reverse primer 5′-accctgtggtccaacgactcctctc-3′. All real-time RT-PCRs were performed in duplicate, and the data are presented as mean ± SD.

Western Blot Analysis

The proteins of tissues were fractionated by electrophoresis on 10 % SDS-polyacrylamide gel and electro-blotted to polyvinylidene difluoride (PVDF) filter membranes for 2 h at 200 V. The PVDF membranes were incubated with blocking buffer (TBST, 50 mM Tris–HCl, pH 7.4, 150 mM NaCl, 0.1 % Tween-20, 50 % skimmed milk) for 1 h at room temperature, followed by overnight treatment with the primary antibody at 4 °C, and then with an HRP-conjugated secondary antibody. After washing, the reactive bands were detected by ECL. Immunoblotting was performed with goat polyclonal to TIMP-1 (R&D, 1:500), rabbit polyclonal to MMP9 (Abcam, 1:500), and rabbit monoclonal to β-actin (Abcam, 1:500) primary antibodies. Membranes were subsequently probed with horseradish peroxidase-conjugated secondary antibody (1:5,000; Roche), developed by chemiluminescence and exposed to X-ray film. Densitometry was performed with gel imaging system (Alpha imager 2200, Pharmacia Biotech Co., USA).

Immunohistochemistry

Renal tissue sections at 4 μm were used to perform immunohistochemical staining for ColIV and FN with rabbit polyclonal to ColIV antibody (1:500; Abcam) and rabbit polyclonal to FN antibody(1:500; Abcam). Color was developed by incubating with diaminobenzidine and counterstaining with hematoxylin. For semiquantitative analysis, 20 high-power microscope fields were randomly selected, and the pathological image analysis was used to calculate the positive-staining signal percentage with image-pro plus 6.0 software.

Statistical Analysis

Statistical analysis was performed using the SPSS16.0 software. Values are expressed as mean ± SD. Differences/correlations between groups were calculated with Student's t test, and Pearson's correlation test. $P < 0.05$ was defined as being significant.

Results

The Expression and Location of miR-21 in Renal Tissue

To determine the localization and distribution of the expression of miR-21, we performed ISH assays. As shown in Fig. 1, miR-21 was primarily located in the cortex, with minimal expression in the medulla and papilla of the kk-ay kidneys. The expression of miR-21 was strikingly enhanced in kidneys with kk-ay mice for 20 weeks of age, compared with the normal C57BL kidneys (Fig. 1a). Furthermore, we found that the enhanced expression of miR-21 was localized mainly in glomerular and renal tubular cells within the cortex, medulla, and papilla of the kidneys of kk-ay mice (Fig. 1b). Next, to further identify the difference of miR-21 expression between kk-ay diabetic mice and normal C57BL, we measured the expression of miR-21 by real-time qRT-PCR (Fig. 1c) at different ages. At 8 weeks of age, there was no significant difference for miR-21 expression between kk-ay diabetic mice and normal C57BL (Fig. 1c). At 16 weeks of age, the expression of miR-21 was markedly increased in kk-ay diabetic mice. With the progression of DN, the expression of miR-21 was further elevated in kk-ay diabetic mice at 20 weeks of age; the expression in kk-ay was significantly higher than that in C57BL ($P < 0.01$), consistent with the result ISH. Taken together, our result suggested that the expression of miR-21 was significantly increased in diabetic kidney. Thus, we concluded that miR-21 may play a role in the pathogenesis of DN.

The Correlation Between miR-21 and ACR, Creatine Clearance Ratio

ACR has been demonstrated to be a good clinical predictor of renal lesions in DN [25]. Creatinine clearance ratio (Ccr), which is generally considered as marker of renal function, reflects renal filtration function. To evaluate whether miR-21 could affect ACR and Ccr, we examined them at different ages from 8 to 20 weeks. At 8 weeks of age, compared with c57B mice, ACR, Ccr, and miR-21 expression in kk-ay mice were not significantly different (Figs. 1c, 2a, b). At 16–20 weeks of age, with the progression of DN, the ACR began to increase and the Ccr began to decline, the expression of miR-21 was elevated to high level. Overall, miR-21 expression was positively correlated with ACR ($r = 0.970$, $P = 0.006$; Fig. 2c) and negatively correlated with Ccr ($r = -0.950$, $P < 0.01$; Fig. 2f). Interestingly, HbA1C and total cholesterol (T-Cho) were found to be significantly higher in kk-ay mice compared with C57BL mice at 20 weeks of age. However, there was no correlation between miR-21 and T-Cho, HbA1C (data not shown). Next, we further evaluated whether inhibition of miR-21 was able to reduce urine albumin excretion and ameliorate renal function. kk-ay mice were injected intraperitoneally with antagomir-21(miR-21 antagonist) for 8 weeks, we found that there was a significant decrease of ACR and an increase in Ccr in antagmiR-21 group compared with kk-ay mice (Fig. 2d, e; $P < 0.05$). Together; our results suggested that miR-21 may increase urine protein excretion and aggravate renal function injury, and that antagomir-21 may have renoprotective effects under diabetic conditions.

The Relationship Between miR-21 and Morphological Changes

It was well known that excessive accumulation of ECM leads to glomerulosclerosis and renal fibrosis [3]. GSI generally considered as a marker of the degree of renal fibrosis [26]. Therefore, to evaluate whether miR-21 plays a role in renal fibrosis in DN, renal morphology was observed by light and electronic microscopy at 20 weeks of age. As shown in Fig. 3, HE staining showed that increased mesangial matrix and greater segment glomerulosclerosis in kk-ay mice (Fig. 3a, b); Masson staining demonstrated that the amount of collagen fibers (Fig. 3d, e) and renal fibrosis score in kk-ay mice were significantly higher in glomerular regions compared with that in C57BL mice at 20 weeks of age (0.22 ± 0.13 vs. 0.11 ± 0.09; $P < 0.05$). Electron microscope exhibited thickening of GBM (0.416 ± 0.019 vs. 0.185 ± 0.008 μm; $P < 0.05$) and foot process fusion in diabetic mice (Fig. 3g, h). Interestingly, the expression level of miR-21 was positively correlated with glomerular fibrosis index (GSI) and GBM (Pearson correlation, $r_{GSI} = 0.870$, $r_{GBM} = 0.830$, $P < 0.05$); Furthermore, after 8 weeks of treatment of antagomir-21, glomerular fibrosis index (GSI) and GBM were slightly but significantly decreased in the kk-ay diabetic mice (Fig. 3c, f, i–k; $P < 0.05$). This result suggests that miR-21 may promote renal fibrosis in diabetic mice, and inhibiting miR-21 can slightly ameliorate renal fibrosis.

The Correlation Between MMP-9/TIMP1 and miR-21 Expression

MMPs and TIMPs play a critical role in extra cellular matrix (ECM) homeostasis, and deregulated ECM remodeling

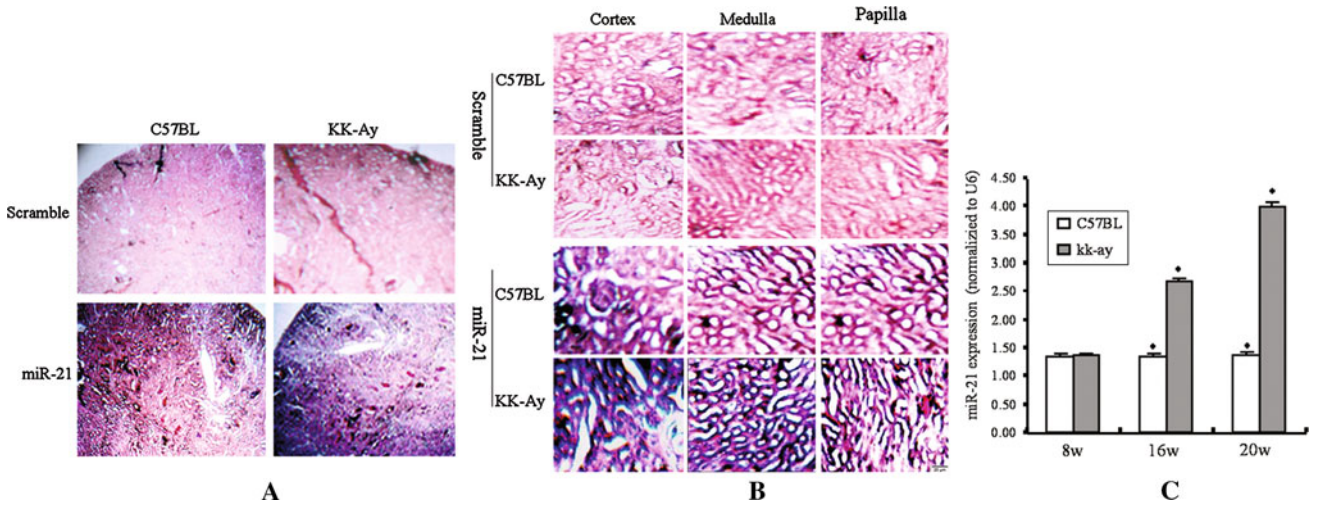

Fig. 1 ISH and real-time quantitative RT-PCR showed that the location and expression of miR-21 in normal C57BL and kk-ay mice kidneys. **a** The location and distribution of miR-21 in normal C57BL and kk-ay mice kidney at 20 weeks of age. Compared with the normal C57BL, the expression of miR-21 was strikingly enhanced in kidneys with kk-ay mice (*blue* staining showed the presence of miR-2). **b** miR-21 was primarily expressed in the cortex, medulla, and papilla of kk-ay kidney. **c** Levels of miR-21 expression in kk-ay mice and normal C57BL as measured by qRT-PCR ($P < 0.01$). Mean ± SD of triplicate measurements (Color figure online)

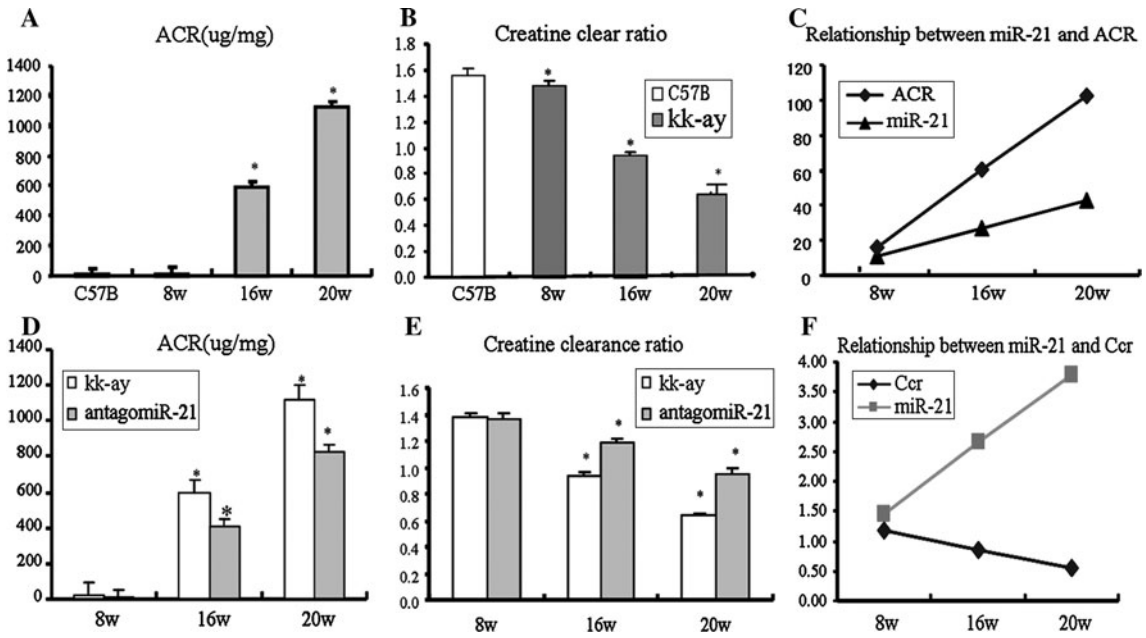

Fig. 2 With the process of diabetic nephropathy, the urine albumin excretion rate in kk-ay mice was markedly increased compared with C57BL mice (**a** $P < 0.05$), whereas Ccr was gradually decreased (**b** $P < 0.05$). After antagomir-21 treatment, there was a significant decrease of ACR (**d** $P < 0.05$) and an increase in Ccr (**e** $P < 0.05$) at 20 weeks of age ($P < 0.05$). miR-21 was positively correlated with ACR (**c**), and negatively correlated with Ccr (**f**)

contributes to renal fibrosis [3]. According to microRNA targets predicted (http://www.diana.cslab.ece.ntua.gr/, http://www.microrna.org, and http://www.targetscan.org), MMP-9 was a validated target of miR-21 (Fig. 4a). Thus, we speculated that miR-21 may downregulate MMP-9 expression and lead to the increase of TIMP1. To determine whether miR-21 regulate the expression of MMP-9/TIMP1 mRNA and protein, real-time RT-PCR and western blot were used in renal tissues to measure MMP-9/TIMP1 mRNA and protein level. Real-time RT-PCR and western blot results showed that the level of TIMP-1 mRNA and protein were significantly increased in kk-ay mice (At 20 weeks of age) compared with control C57BL mice (Fig. 4b, c; $P < 0.05$). In contrast, MMP-9 mRNA and protein level were significantly decreased compared with control C57BL mice (Fig. 4c, d; $P < 0.05$). Interestingly, miR-21 expression positively correlated with

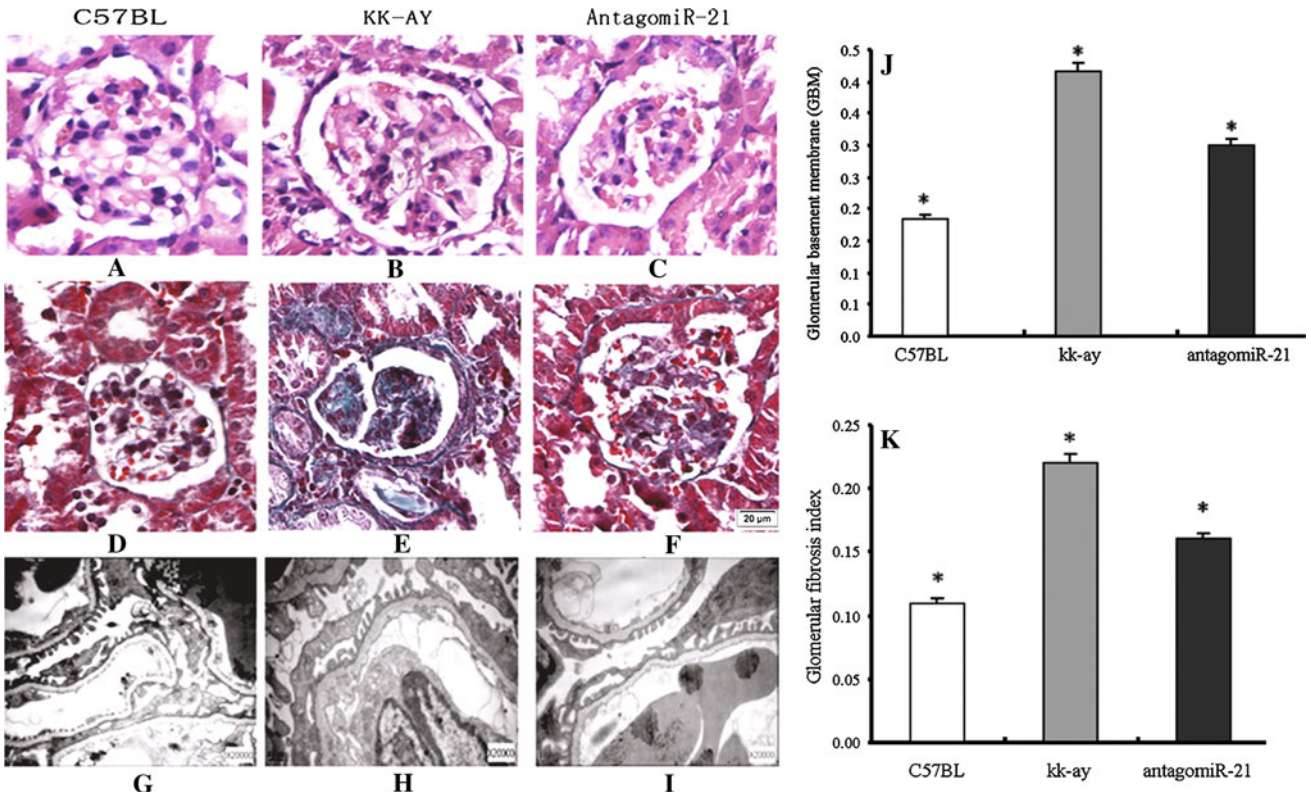

Fig. 3 Morphological changes of renal tissue sections at 20 weeks of age. Representative photographs of kidney section from normal C57BL mice showed that mesangial matrix, glomerular basement membrane (GBM) (**a**, **d**, **g**). Diffuse expansion of mesangial matrixes, thickening of the GBM, foot process fusion, and glomerular fibrosis score were observed in kk-ay mice (**b**, **e**, **h** $P < 0.05$). Masson's trichrome-stained demonstrate cross-linked collagen (*blue*) in the glomerular regions of kk-ay kidneys (**e**, **f**). Thickening of the basement membrane (GBM) in kk-ay mice was significantly compared with that in C57BL mice at 20 weeks of age (**g**, **h**). After antagmir-21 treatment, GSI and GBM were slightly decreased in kk-ay mice (**c**, **f**, **i**–**k** $P < 0.05$, ×400) (Color figure online)

TIMP1 protein (Fig. 4e; Pearson correlation, $r = 0.941$, $P < 0.05$), and negatively correlated with MMP-9 protein (Fig. 4e; Pearson correlation, $r = -0.801$, $P < 0.05$). Importantly, antagmir-21 decreased TIMP1 and increased MMP-9 protein level. These data indicated that miR-21 may directly downregulate MMP-9 protein expression and indirectly lead to the increase of TIMP1.

The Effect of miR-21 on Collagen IV and Fibronectin

Marked accumulation of ECM is a histological hallmark of DN that leads to renal fibrosis and end-stage kidney disease [3]. To explore whether miR-21 affected ColIV and FN, we examined ColIV and FN mRNA and proteins of renal tissues by real-time RT-PCR and immunohistochemical staining, respectively. Immunohistochemical staining exhibited that ColIV and FN were localized in the glomerular areas (Fig. 5d), and mean optical density value of ColIV and FN in kk-ay mice were significantly higher than that in C57BL mice at 20 weeks of age (Fig. 5a, b; $P < 0.05$). Furthermore, real-time RT-PCR showed that ColIV and FN mRNA were remarkably increased in diabetic kidneys compared with C57BL (Fig. 5c; $P < 0.05$), consistent with ColIV and FN proteins results. The expression of miR-21 was found to positively correlate with ColIV and FN proteins (Pearson correlation, $r_{\text{ColIV}} = 0.832$, $r_{\text{FN}} = 0.714$, $P < 0.05$). Next, we determined whether antagmiR-21 is sufficient to suppress the mRNA and protein expression of ColIV and FN. For this purpose, kk-ay DN mice were injected intraperitoneally with antagomir-21 (30 mg/kg day) for 8 weeks, we found that the mRNA and protein level of ColIV and FN in antagomiR-21 group were significantly decreased compared with kk-ay diabetic mice without treatment (Fig. 5a–c; $P < 0.05$). Taken together, the results suggested that miR-21 contributed to, whereas antagomir-21 ameliorated ECM production in diabetic kidneys.

Discussion

DN is a major microvascular complication and a leading cause of chronic kidney failure in individuals with diabetes [27, 28]. Although high blood glucose, high blood pressure,

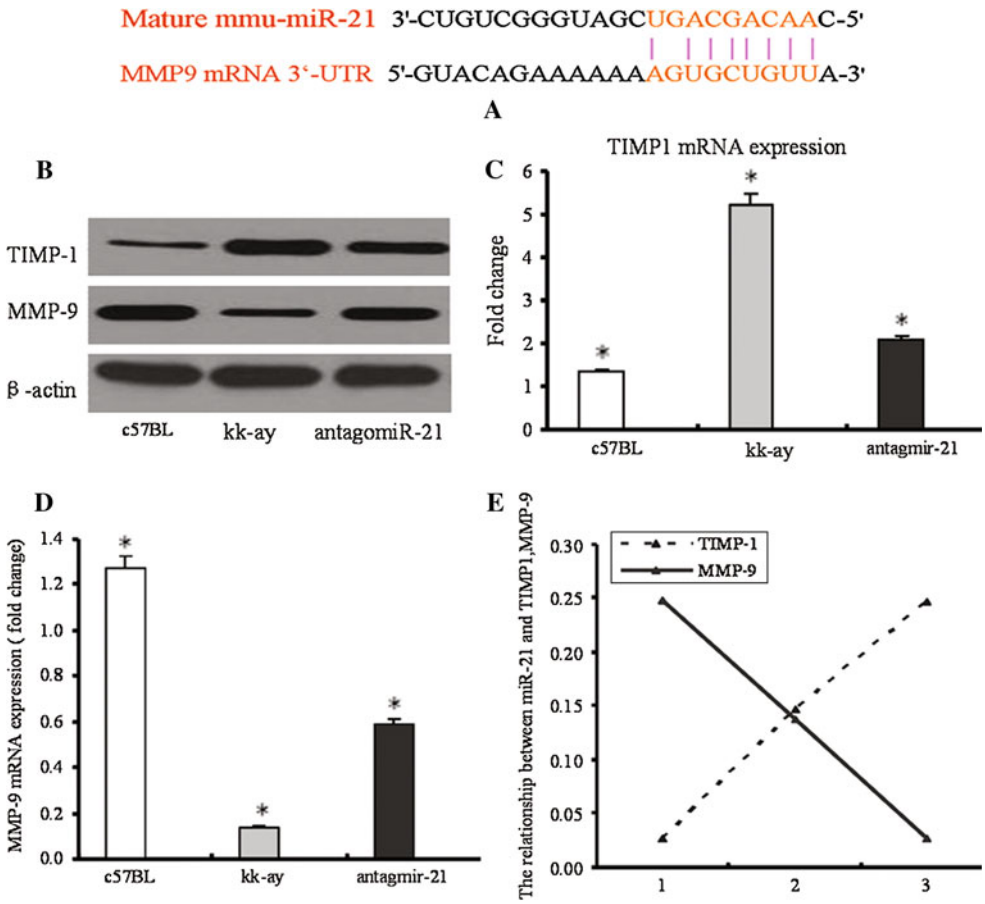

Fig. 4 TIMP1 and MMP9 mRNA and protein expression in the kidneys of 20-week mice, there were statistically significant increase in the expression of TIMP1 mRNA and protein in kk-ay mice comparing with C57BL. In contrast, MMP9 mRNA and protein levels in kk-ay mice were significantly decreased compared with that in C57BL mice. Antagmir-21 significantly reduced TIMP1 and increased MMP9 protein expression. ($P < 0.05$, compared with control). **a** miR-21 binding region of the 3′-UTR of MMP-9. **b** Western analysis for TIMP1 and MMP9 protein. **c** TIMP1 mRNA expression levels. **d** MMP9 mRNA expression levels. **e** The correlation between miR-21 and MMP-9/TIMP1 protein levels

hemodynamic and metabolic factors, hereditary factors, or family history are involved in the pathogenesis of DN, the exact cause of DN is currently unknown. There is increasing evidence that miRs are involved in the pathogenesis of metabolic diseases such as diabetes mellitus [29–31]. Here, we studied whether miR-21 was involved in the pathogenesis of DN. Our ISH results showed that the expression of miR-21 was strikingly enhanced in kidneys of kk-ay DN mice, the miR-21 was primarily localized in glomerular and renal tubular cells within the cortex, medulla, and papilla. Furthermore, real-time RT-PCR results showed that the expression of miR-21 was markedly increased with the progression of DN, consistent with the ISH results. The likely molecular mechanism of miR-21 overexpression was that hyperglycemia led to the increase of TGF-β1/Smad3, which then promoted miR-21 overexpression [32, 33]. Interestingly, the expression of miR-21 was positively correlated with ACR and glomerular fibrosis index (GSI), and negatively correlated with Ccr. Most importantly, antagomir-21 attenuated albuminuria and ameliorated renal function in DN mice. However, our results were different from the previous results by Zhang et al. [34], which showed miR-21 expression was down regulated in response to early DN, and that overexpression of miR-21-inhibited proliferation of mesangial cells and decreased the 24-h urine albumin excretion rate in early diabetic db/db mice. The most possible reason of the experimental inconsistence was that our animal model and the stage of DN mice were different from Zhang et al. Our kk-ay DN mice were in the later stage of DN (at 16–20 weeks of age), while diabetic db/db mice from Zhang et al. were in the early stage of DN (at 4 weeks of age). Thus, we conclude that miR-21 is involved in the process of DN, which promote urinary protein excretion and aggravate renal function injury.

MMPs are a family of functionally related zinc-containing enzymes that include interstitial collagenases, gelatinases, stromelysin, matrilysin, metalloelastase, and membrane-type MMPs [35]. The relative balance of MMPs and TIMPs is thought to determine the rate of ECM turnover, so that even slight deviations in gene expression can contribute to the progression of some diseases, such as tumor metastasis and renal fibrosis [36]. Increasing evidence indicates that MMP-9 and TIMP-1 were involved in the pathogenesis of DN. High glucose decreased MMP-9 production and increased TIMP-1 expression in podocytes, which contributed to the GBM abnormality and proteinuria caused by an imbalance in ECM synthesis and degradation

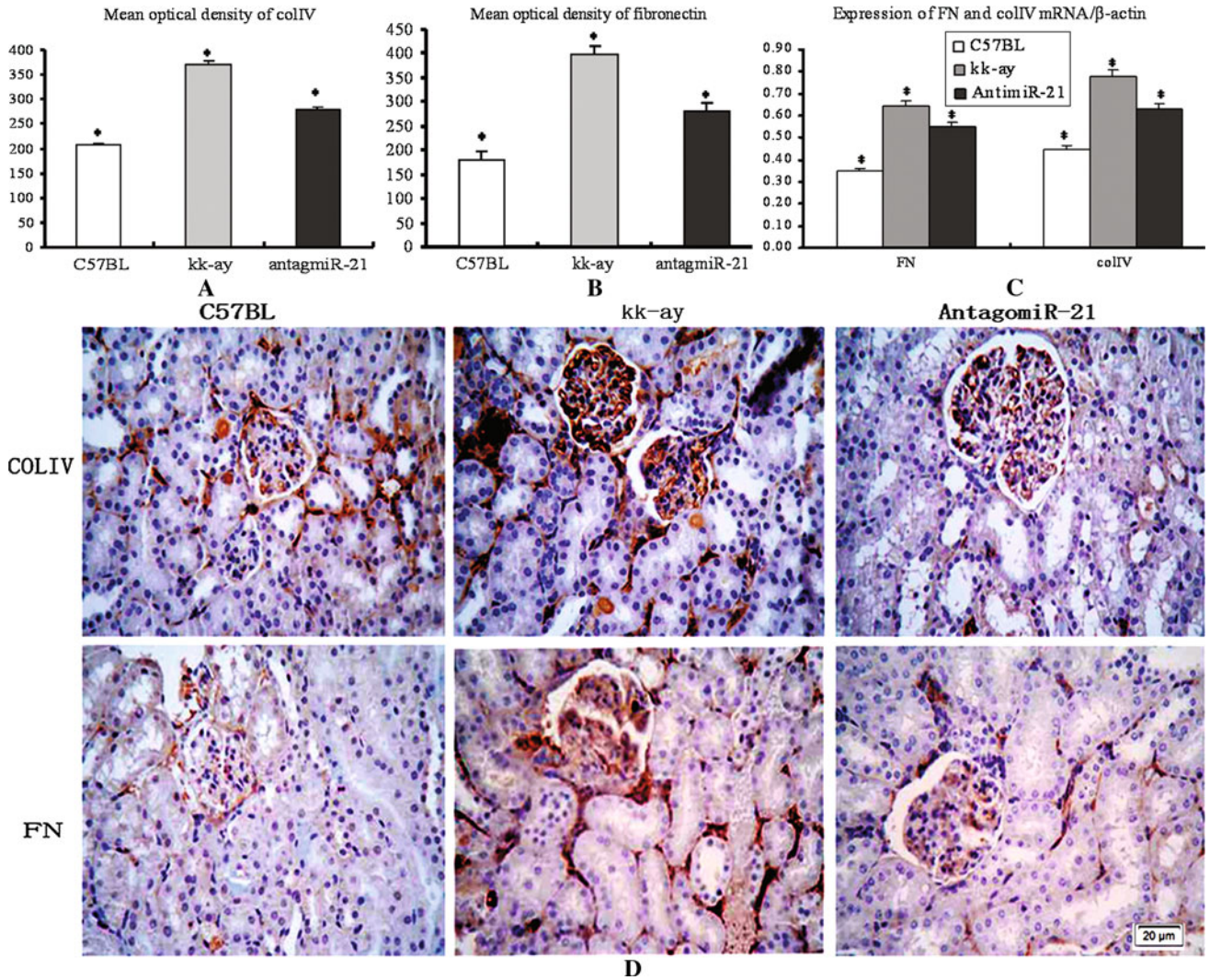

Fig. 5 ColIV and FN mRNA and protein expression in the kidneys of 20-week mice. **a** Mean optical density value of ColIV in kk-ay mice was significantly higher than that in C57BL mice at 20 weeks of age ($P < 0.05$). AntagomiR-21 remarkably decreased ColIV protein levels ($P < 0.05$). **b** Mean level of FN in kk-ay mice was markedly increased comparing with that in C57BL mice ($P < 0.05$). AntagomiR-21 also significantly decreased FN protein levels ($P < 0.05$). **c** Expression of FN and ColIV mRNA, there was markedly increase in kk-ay mice compared with in C57BL mice ($P < 0.05$). AntagomiR-21 significantly decreased FN and ColIV mRNA levels ($P < 0.05$). **d** ColIV and FN were localized in the glomerular areas, with stronger staining intensity in kk-ay mice. The staining of ColIV and FN in kk-ay mice was stronger than that in C57BL mice, ×400

[37]. Although numerous studies showed that miR-21 can downregulate MMPs and upregulate TIMP expression [16–19], whether miR-21 regulate the balance of MMP-9 and TIMP-1 in DN remain unclear. Since MMP-9 was a validated target of miR-21 [16, 17], it is tempting to speculate that overexpression of miR-21 might downregulate MMP-9 expression and alter the balance of MMP-9/TIMP1. In our experiment, we found that miR-21 expression negatively correlated with MMP-9 expression, and antagmir-21 increased MMP-9 mRNA and protein expression, suggesting that miR-21 directly regulated MMP-9. Meantime, the expression level of TIMP-1 mRNA and protein were remarkably increased in diabetic mice, and that miR-21 positively correlated with TIMP-1 expression. These results were consistent with the previous research results [15, 16, 19, 36]. Together, our results suggested that miR-21 directly downregulated MMP-9 and indirectly increased TIMP-1 expression, which contributed to ECM synthesis and renal fibrosis.

Earlier reports showed that excessive ECM proteins were deposited in the mesangium and basement membrane of the glomerulus in DN [3]. This process alters kidney structure, and adversely affects the function of kidney function. ECM of the diabetic kidney is subjected to a balanced turnover: on the one hand, new ECM components are synthesized by mesangial cells and fibroblasts; on the

other hand, ECM components are continuously degraded by the action of a family of MMPs. The accumulation of ECM proteins in DN has been attributed to an imbalance in the ratio of MMPs to their inhibitors (TIMP) in favor of reduced proteolytic activity, and excessive accumulation of ECM leads to renal fibrosis [3]. There is currently no definitive treatment for renal fibrosis. Recent studies showed that miR-21 regulates both lung and heart fibrosis by enhancing the fibrogenic activity or promoting the proliferation of interstitial fibroblasts [38, 39]. In this experiment, we evaluated the effect of miR-21 on ECM production by real-time RT-PCR and immunohistochemical staining. Meanwhile, the correlation between miR-21 and ECM was analyzed by Pearson correlation. Our result showed that ColIV and FN were remarkably increased in kk-ay DN. Furthermore, the expression of miR-21 was positively correlated with ColIV and FN proteins. In contrast, antagomir-21 decreased ColIV and FN proteins. Taken together, the results suggested that miR-21 causes, whereas inhibiting of the endogenous miR-21 ameliorates, collagen, and FN accumulation in diabetic kidneys. It is also likely that miR-21 is able to contribute to the increase of TIMP-1 protein and the decrease of MMP-9 protein, which leads to deposition of ECM components. Thus, we speculated that miR-21 promotes ECM deposition by regulating the expression of TIMP-1 and MMP-9 in DN, and blocking miR-21 may be a novel therapeutic target to ameliorate renal fibrosis.

In summary, our study suggests that miR-21 is involved in the pathogenesis of DN, and that the effect of miR-21 on renal fibrosis is via the regulation of MMP-9 and TIMP-1 expression. Inhibition of miR-21 may be a therapeutic approach to suppress renal fibrosis.

Limitation

Human DN is very complicated microvascular complications of diabetes, and this kk-ay animal model of human DN only partly simulated pathological and functional changes [4]. Thus, further studies with other animal models of DN and human studies are needed to confirm the role of miR-21 in the pathogenesis of DN.

Acknowledgments This study was supported by Grants from the Major National Basic Research Program of China (973 Program, No. 2012CB518602), the National Natural Science Foundation of China (No. 81173238), and Scientific Research Project of Beijing Educational Committee (No. KZ201110025025).

References

1. Rychlik, I., Miltenberger-Miltenyi, G., & Ritz, E. (1998). The drama of the continuous increase in end-stage renal failure in patients with type II diabetes mellitus. *Nephrology, Dialysis, Transplantation, 13*(Suppl 8), 6–10.
2. Tervaert, T. W., Mooyaart, A. L., Amann, K., et al. (2010). Pathologic classification of diabetic nephropathy. *Journal of the American Society of Nephrology, 21*, 556–563.
3. Mason, R. M., & Wahab, N. A. (2003). Extracellular matrix metabolism in diabetic nephropathy. *Journal of the American Society of Nephrology, 14*, 1358–1373.
4. Ito, T., Tanimoto, M., Yamada, K., et al. (2006). Glomerular changes in the KK-Ay/Ta mouse: A possible model for human type 2 diabetic nephropathy. *Nephrology (Carlton), 11*, 29–35.
5. Perron, M. P., & Provost, P. (2008). Protein interactions and complexes in human microRNA biogenesis and function. *Frontiers in Bioscience, 13*, 2537–2547.
6. Poy, M. N., Eliasson, L., Krutzfeldt, J., et al. (2004). A pancreatic islet-specific microRNA regulates insulin secretion. *Nature, 432*, 226–230.
7. Kloosterman, W. P., Lagendijk, A. K., Ketting, R. F., et al. (2007). Targeted inhibition of miRNA maturation with morpholinos reveals a role for miR-375 in pancreatic islet development. *PLoS Biology, 5*, e203.
8. El Ouaamari, A., Baroukh, N., Martens, G. A., et al. (2008). miR-375 targets 3′-phosphoinositide-dependent protein kinase-1 and regulates glucose-induced biological responses in pancreatic beta-cells. *Diabetes, 57*, 2708–2717.
9. Tang, X., Muniappan, L., Tang, G., et al. (2009). Identification of glucose-regulated miRNAs from pancreatic beta cells reveals a role for miR-30d in insulin transcription. *RNA, 15*, 287–293.
10. He, A., Zhu, L., Gupta, N., et al. (2007). Overexpression of micro ribonucleic acid 29, highly up-regulated in diabetic rats, leads to insulin resistance in 3T3-L1 adipocytes. *Molecular Endocrinology, 21*, 2785–2794.
11. Qin, W., Chung, A. C., Huang, X. R., et al. (2011). TGF-beta/Smad3 signaling promotes renal fibrosis by inhibiting miR-29. *Journal of the American Society of Nephrology, 22*, 1462–1474.
12. Chung, A. C., Huang, X. R., Meng, X., et al. (2010). miR-192 mediates TGF-beta/Smad3-driven renal fibrosis. *Journal of the American Society of Nephrology, 21*, 1317–1325.
13. Wang, Q., Wang, Y., Minto, A. W., et al. (2008). MicroRNA-377 is up-regulated and can lead to increased fibronectin production in diabetic nephropathy. *FASEB Journal, 22*, 4126–4135.
14. Zhang, Z., Luo, X., Ding, S., et al. (2012). MicroRNA-451 regulates p38 MAPK signaling by targeting of Ywhaz and suppresses the mesangial hypertrophy in early diabetic nephropathy. *FEBS Letters, 586*, 20–26.
15. Shantikumar, S., Caporali, A., & Emanueli, C. (2012). Role of microRNAs in diabetes and its cardiovascular complications. *Cardiovascular Research, 93*, 583–593.
16. Moriyama, T., Ohuchida, K., Mizumoto, K., et al. (2009). MicroRNA-21 modulates biological functions of pancreatic cancer cells including their proliferation, invasion, and chemoresistance. *Molecular Cancer Therapeutics, 8*, 1067–1074.
17. Gabriely, G., Wurdinger, T., Kesari, S., et al. (2008). MicroRNA 21 promotes glioma invasion by targeting matrix metalloproteinase regulators. *Molecular and Cellular Biology, 28*, 5369–5380.
18. Roy, S., Khanna, S., Hussain, S. R., et al. (2009). MicroRNA expression in response to murine myocardial infarction: miR-21 regulates fibroblast metalloprotease-2 via phosphatase and tensin homologue. *Cardiovascular Research, 82*, 21–29.
19. Meng, F., Henson, R., Wehbe-Janek, H., et al. (2007). MicroRNA-21 regulates expression of the PTEN tumor suppressor gene in human hepatocellular cancer. *Gastroenterology, 133*, 647–658.
20. Li, H. Y., Hou, F. F., Zhang, X., et al. (2007). Advanced oxidation protein products accelerate renal fibrosis in a remnant

kidney model. *Journal of the American Society of Nephrology, 18*, 528–538.
21. Miyazaki, T., Aoyama, I., Ise, M., et al. (2000). An oral sorbent reduces overload of indoxyl sulphate and gene expression of TGF-beta1 in uraemic rat kidneys. *Nephrology, Dialysis, Transplantation, 15*, 1773–1781.
22. Nuovo, G. J. (2008). In situ detection of precursor and mature microRNAs in paraffin embedded, formalin fixed tissues and cell preparations. *Methods, 2008*(44), 39–46.
23. Schmittgen, T. D., Lee, E. J., Jiang, J., et al. (2008). Real-time PCR quantification of precursor and mature microRNA. *Methods, 44*, 31–38.
24. Pfaffl, M. W. (2001). A new mathematical model for relative quantification in real-time RT-PCR. *Nucleic Acids Research, 2001*(29), e45.
25. Viberti, G., & Wheeldon, N. M. (2002). Microalbuminuria reduction with valsartan in patients with type 2 diabetes mellitus: A blood pressure-independent effect. *Circulation, 106*, 672–678.
26. Fioretto, P., & Mauer, M. (2010). Diabetic nephropathy: Diabetic nephropathy-challenges in pathologic classification. *Nature Reviews Nephrology, 6*, 508–510.
27. Krolewski, A. S., Canessa, M., Warram, J. H., et al. (1988). Predisposition to hypertension and susceptibility to renal disease in insulin-dependent diabetes mellitus. *New England Journal of Medicine, 318*, 140–145.
28. Ballard, D. J., Humphrey, L. L., Melton, L. J., 3rd, et al. (1988). Epidemiology of persistent proteinuria in type II diabetes mellitus. Population-based study in Rochester, Minnesota. *Diabetes, 37*, 405–412.
29. Krichevsky, A. M., & Gabriely, G. (2009). miR-21: A small multi-faceted RNA. *Journal of Cellular and Molecular Medicine, 13*, 39–53.
30. Zarjou, A., Yang, S., Abraham, E., et al. (2011). Identification of a microRNA signature in renal fibrosis: Role of miR-21. *American Journal of Physiology: Renal Physiology, 301*, F793–F801.
31. Chau, B. N., Xin, C., Hartner, J., et al. (2012). MicroRNA-21 promotes fibrosis of the kidney by silencing metabolic pathways. *Science Translational Medicine, 4*, 121ra118.
32. Chen, S., Hong, S. W., Iglesias-de la Cruz, M. C., et al. (2001). The key role of the transforming growth factor-beta system in the pathogenesis of diabetic nephropathy. *Renal Failure, 2001*(23), 471–481.
33. Davis, B. N., Hilyard, A. C., Lagna, G., et al. (2008). SMAD proteins control DROSHA-mediated microRNA maturation. *Nature, 454*, 56–61.
34. Zhang, Z., Peng, H., Chen, J., et al. (2009). MicroRNA-21 protects from mesangial cell proliferation induced by diabetic nephropathy in db/db mice. *FEBS Letters, 583*, 2009–2014.
35. Snoek-van Beurden, P. A., & Von den Hoff, J. W. (2005). Zymographic techniques for the analysis of matrix metalloproteinases and their inhibitors. *BioTechniques, 2005*(38), 73–83.
36. Suminoe, A., Matsuzaki, A., Hattori, H., et al. (2007). Expression of matrix metalloproteinase (MMP) and tissue inhibitor of MMP (TIMP) genes in blasts of infant acute lymphoblastic leukemia with organ involvement. *Leukemia Research, 31*, 1437–1440.
37. Bai, Y., Wang, L., Li, Y., et al. (2006). High ambient glucose levels modulates the production of MMP-9 and alpha5(IV) collagen by cultured podocytes. *Cellular Physiology and Biochemistry, 17*, 57–68.
38. Liu, G., Friggeri, A., Yang, Y., et al. (2010). miR-21 mediates fibrogenic activation of pulmonary fibroblasts and lung fibrosis. *Journal of Experimental Medicine, 207*, 1589–1597.
39. Thum, T., Gross, C., Fiedler, J., et al. (2008). MicroRNA-21 contributes to myocardial disease by stimulating MAP kinase signalling in fibroblasts. *Nature, 456*, 980–984.